IEEE Access
Multidisciplinary | Rapid Review | Open Access Journal

Received March 14, 2019, accepted April 30, 2019, date of publication May 7, 2019, date of current version May 20, 2019.

Digital Object Identifier 10.1109/ACCESS.2019.2915092

Design of Novel Reconfigurable Filter With Simultaneously Tunable and Switchable Passband

YU-JING ZHANG[1], JING CAI[2], AND JIAN-XIN CHEN[1,3], (Senior Member, IEEE)
[1]School of Information Science and Technology, Nantong University, Nantong 226019, China
[2]Affiliated Hospital of Nantong University, Nantong University, Nantong 226001, China
[3]Nantong Research Institute for Advanced Communication Technologies, Nantong 226019, China

Corresponding author: Jing Cai (caijing2005@163.com)

This work was supported in part by the Natural Science Foundation of Jiangsu Province under Grant BK20161281, and in part by the Science-Technology Programs of Nantong under Grant MS12018004.

ABSTRACT This paper presents a new loading scheme for adding the varactor and PIN diodes into a quarter-wavelength ($\lambda/4$) resonator. Based on this, a novel reconfigurable filter with simultaneously tunable and switchable passband is introduced. Constant absolute bandwidth (ABW) and two transmission zeroes (TZs) can be obtained to enhance the passband performance in the ON-state. As the passband is turned to the OFF-state, high isolation can be realized at the frequency of interest. Meanwhile, the varactors, which are used to control the external quality factor (Q_e) in the ON-state, can be tuned to improve the in-band isolation in the OFF-state. For demonstration, a reconfigurable filter with tunable and switchable passband is fabricated and measured. The measured results show a high selectivity tunable passband with the tuning range of 32.4% and 3-dB ABW of 51 ± 2 MHz in the ON-state. The isolation >40dB can be achieved in the OFF-state. Good agreement of the simulated and measured results is presented to verify the theoretical predictions.

INDEX TERMS Reconfigurable filter, PIN diode, varactor diode, quarter-wavelength ($\lambda/4$) resonator.

I. INTRODUCTION

Modern wireless communication systems frequently demand the components with reconfigurability to realize more functions within the limited circuit space or cost. Various kinds of reconfigurable components, such as power divider [1]–[4], coupler [5], [6], duplexer [7], antenna [8], [9], and filter [10]–[12] have been studied to satisfy the application requirements of RF front-ends. In among, bandpass filter (BPF), as one of the most important devices that can transmit interested signal and eliminate unwanted interference, play a key role in the communication system. Hence, the BPF possessing various reconfigurabilities have been deeply studied in recent years [10]–[39].

The reconfigurable BPF generally indicates that the variable units, such as microelectromechanical system (MEMS) [13], [14], ferroelectric [15], [16], microfluidic [17] and semiconductor diodes (varactor and PIN) [18]–[21], are inserted into the transmission line resonator so as to obtain the reconfigurability. Meanwhile, the resonator can be constructed by the different topologies and technologies such as substrate integrated waveguide (SIW) [22], [23], dielectric resonator [24], lumped elements [25] and microstrip [26]–[30]. In among, loading semiconductor diodes (varactor or PIN) into the microstrip filters is one of the easiest and cheapest ways to realize the reconfigurability.

The researches on the reconfigurable BPF in the academic and industrial fields mainly concentrated on two aspects: tunability and switchability. The tunability generally indicates the passband tunability which can be realized by using the tunable units to tune the center-frequency or the bandwidth of passband. To the other aspect, the switchability can be also divided into two categories. The first is that using the switchable units to switch on or off the passband [26], [31], [32]. The second mainly employs the switchable units to realize the transformation between different filtering responses (bandpass or bandstop) in a single circuit [33], [34]. As the evolving of the RF systems towards the higher integration level, the devices with more functions are highly desirable. Accordingly, the studies of multifunctional reconfigurable filters are carried out. For example, the tunability for both frequency and bandwidth of the passband can be integrated in a BPF by loading more varactors to the resonator [35], [36].

The associate editor coordinating the review of this manuscript and approving it for publication was Vincenzo Conti.

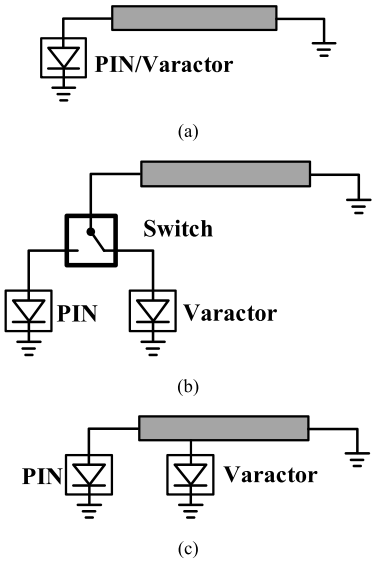

FIGURE 1. Layout of the element-loaded λ/4 UIR (a) loading the PIN or varactor at the open end of the λ/4 UIR, (b) using an extra SPDT switch to load the PIN and varactor at the open end of the λ/4 UIR simultaneously, (c) varactor-PIN-loaded λ/4 UIR using new loading scheme.

However, few studies about the switchability of the tunable passband are reported so far.

In this paper, a reconfigurable filter with simultaneously tunable and switchable passband is proposed by using reconfigurable quarter-wavelength (λ/4) uniformed-impedance resonator (UIR). The frequency-tuning passband is realized by the varactors loaded on the specific position of the UIR, and can be turned to the ON- or OFF-state in each operation frequency controlled by the PIN diode at the UIR end. In order to make the filter more attractive, two extra varactors and source-to-load (S-L) coupling structure are added into the feeding structure for realizing constant absolute bandwidth (ABW) and two transmission zeroes (TZs) associating with the tunable passband during the frequency-agile process of the passband. When the filter works in the OFF-state, the in-band isolation can be optimized and improved by the varactors in the feeding structure.

II. RECONFIGURABLE λ/4 RESONATOR USING NEW LOADING SCHEME

In order to integrate the tunability and switchability of the passband into a single filter, a new resonator, which possesses these two reconfigurabilities simultaneously, should be investigated. In the previous designs of the tunable/switchable BPFs, the λ/2 and λ/4 resonators are widely used [31]–[36], especially for the λ/4 resonator which is a minimum-size element. Fig. 1(a) shows a traditional element-loaded λ/4 UIR, and the PIN or varactor is generally loaded at its open end. This is because the open end of the UIR is with the maximum RF distribution voltage so that the controlling effect of the PIN/varactor is optimum. If the UIR wants to own the tunability and switchability of the fundamental mode (for constructing the passband in the filter design) at the same time, extra single-pole double-throw (SPDT) switch should be added, preceding the varactor and the PIN as shown in Fig. 1(b). The design complexity will increase undoubtedly.

In order to overcome this drawback, a varactor-PIN-loaded λ/4 UIR is introduced, as shown in Fig. 1(c). The PIN is loaded at the open end while the varactor is loaded at a specific position on the UIR, which will be discussed in detail later. When the PIN is turned off, a tunable λ/4 UIR can be obtained. The frequencies of its resonant modes can still be tuned. When the PIN is turned on, the λ/4 UIR will be turned into a λ/2 UIR with two short ends. Thus, the original fundamental resonance will be suppressed. To the authors' best knowledge, both tunability and switchability are integrated in a single resonator, which is the simplest way due to the adoption of new loading scheme.

To study the frequency-tuning mechanism of the loaded λ/4 UIR in Fig. 1(c), the PIN at the UIR end is turned off, and then it can be equivalent to a small resistance and is negligible so that the analysis model is shown in Fig. 2(a). Z_0 and θ_0 represent the characteristic impedance and total electric length of the UIR, respectively. C_{v1} represents the variable capacitance of the varactor for frequency tuning of the resonant modes, and $p = \theta_p/\theta_0$ is defined to express the varactor-loaded position.

In this study, the substrate of *Rogers 4003C* with a dielectric constant of 3.38, a thickness of 0.813 mm and a loss tangent of 0.0027 is used. The variation range of C_{v1} is set from 0.5pF to 3pF. The parameters of the UIR are chosen as $Z_0 = 64\ \Omega$ (corresponding to 1.2 mm width of the microstrip line) and $L_0 = 40$ mm. The input admittance Y_{in} of the UIR can be expressed as [37]:

$$Y_{in} = \frac{-j}{Z_0}\frac{1-\omega C_v Z_0 \tan(\theta_0 - p\theta_0) - \tan(p\theta_0)\tan(\theta_0 - p\theta_0)}{\tan(\theta_0 - p\theta_0) + \tan(p\theta_0)(1-\omega C_v Z_0 \tan(\theta_0 - p\theta_0))}$$
$$\theta_x = \beta L_x = \frac{\sqrt{\varepsilon_{re}}\cdot 2\pi f_i}{c} L_x, \quad x = 0 \text{ or } p,\ i = 1, 3, 5, \ldots \tag{1}$$

where ε_{re} is the effective dielectric constant and β is the propagation constant. The f_i ($i = 1, 3, 5, \ldots$) represents the frequency of the resonant modes.

The tuning range of f_i is defined as

$$R_i = \frac{f_{i\text{high}} - f_{i\text{low}}}{(f_{i\text{high}} + f_{i\text{low}})/2} \tag{2}$$

where $f_{i\text{low}}$ and $f_{i\text{high}}$ represent the lowest and highest f_i when C_{v1} changes from 0.5pF to 3pF, respectively. When $\text{Im}[Y_{in}]$ is equal to 0 (the resonant condition), the frequency-tuning range of the resonant modes against the variation range of C_{v1} under different p can be extracted and plotted.

Fig. 2(b) gives the variations of the UIR fundamental frequency (f_1) and third harmonic (f_3) against C_{v1} under different position p, where f_3 is the lowest-frequency spurious. Table 1 lists the specific values of R_i under different p. It can be found that both R_1 and R_3 achieve the maximum value when $p = 0$ (the varactor is loaded at the open end of the UIR). As p changes from 0 to 1/3, both of them are decreased.

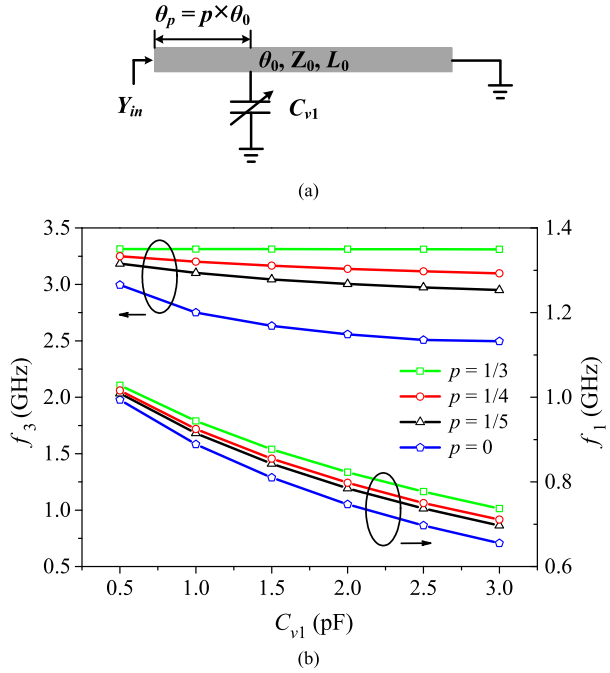

FIGURE 2. Properties of the varactor-loaded λ/4 UIR, (a) layout of the varactor-loaded λ/4 UIR, (b) the variation of f_1 and f_3 versus C_{v1} under different p.

TABLE 1. The tuning range comparison when C_{v1} varies from 0.5 to 3 pF.

p	R_1	R_3
0	41.1%	18.2%
1/5	36.6%	7.6%
1/4	35.3%	4.8%
1/3	33%	0

It is worth to note that when p increases, the R_3 decreases prominently comparing with R_1, which will lead to a wider upper stopband between f_1 and f_3 during the frequency-agile process of the resultant BPF. Thus, $p = 1/5$ is chosen as a tradeoff in terms of frequency-tuning range of f_1 and upper-stopband width in the following design of the reconfigurable filter.

III. DESIGN CONSIDERATION OF PASSBAND TUNABILTY

Fig. 3 shows the structure of the proposed reconfigurable BPF, which consists of two coupled varactor-PIN-loaded λ/4 UIRs, two extra varactors (C_{v2}) added between the input/output feed lines for achieving constant ABW and a pair of shunt stubs between the two feed lines for generating two TZs. The implementation circuit of C_{v1} and C_{v2} is shown in the black dashed line of Fig. 3. The C_{vi} ($i = 1$ or 2) is realized by a lumped capacitor C_{bi} (for DC block) and a varactor C_{ai} in series, and then $C_{vi} = C_{ai}C_{bi}/(C_{ai} + C_{bi})$. The V_{ci} represents the DC bias voltage of the varactor. Since the PIN is a current-controlling diode while the varactor is a voltage-controlling diode, the RF choke (RFC2) for the PIN is an inductor with

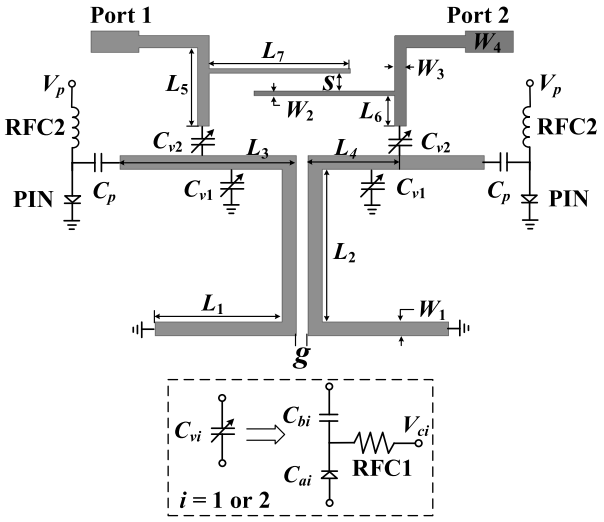

FIGURE 3. The structure of the proposed reconfigurable filter (the varactor bias circuit is in the black dashed line).

56 nH while the RF choke (RFC1) for the varactor is chosen as a cheap resistor with 51 KΩ.

When the bias voltage V_p of the PIN is set as 0V, the PIN is turned off and the end of UIR is open. Under this condition, the passband is in the ON-state and designed to be tunable.

A. CONSTANT ABW OF THE FILTER

In order to realize a tunable BPF with constant ABW, the proposed two UIRs should be coupled and the coupling region should be studied for the sake of obtaining the desired variation trade of coupling coefficient (K_{12}) in the whole frequency-agile range. C_{v2} is employed between feed line and the resonator so that the external quality factor (Q_e) can be tuned. When K_{12} and Q_e are all close to their desired values, constant ABW can be obtained [38].

In this design, a filter is designed with a center frequency of 0.8 GHz and the constant ABW = 51 MHz at initial state ($C_{v1} = 0.5$ pF). Based on the lowpass prototype, the desired values of K_{12} and Q_e can be calculated according to (3) and (4), as given in Fig. 4 and Fig. 5(b).

$$K_{12} = \frac{ABW}{f_0\sqrt{g_1 g_2}} \tag{3}$$

where g_i ($i = 0$, 1 or 2) is the lumped-element value of Chebyshev lowpass prototype response.

$$Q_e = \frac{f_0 g_0 g_1}{ABW} \tag{4}$$

The variation of K_{12} is mainly determined by the coupling region (length of L_2 and width of g) between the two UIRs. In order to extract K_{12}, the following equation should be introduced:

$$K_{12} = \frac{f_{p1}^2 - f_{p2}^2}{f_{p1}^2 + f_{p2}^2} \tag{5}$$

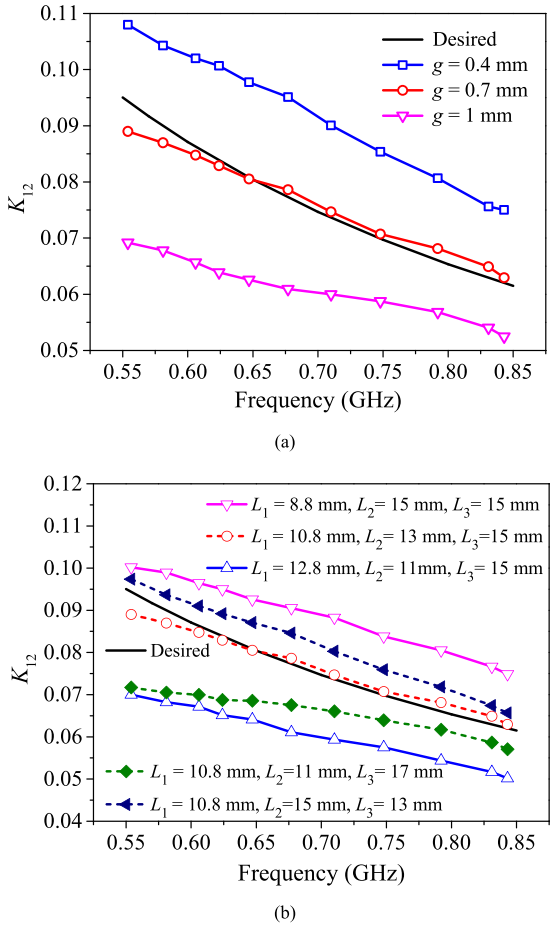

FIGURE 4. Extracted K_{12} versus (a) different g while $L_1 = 10.8$ mm, $L_2 = 13$ mm and $L_3 = 15$ mm are fixed, (b) different L_1, L_2 and L_3 while $g = 0.7$ mm is fixed.

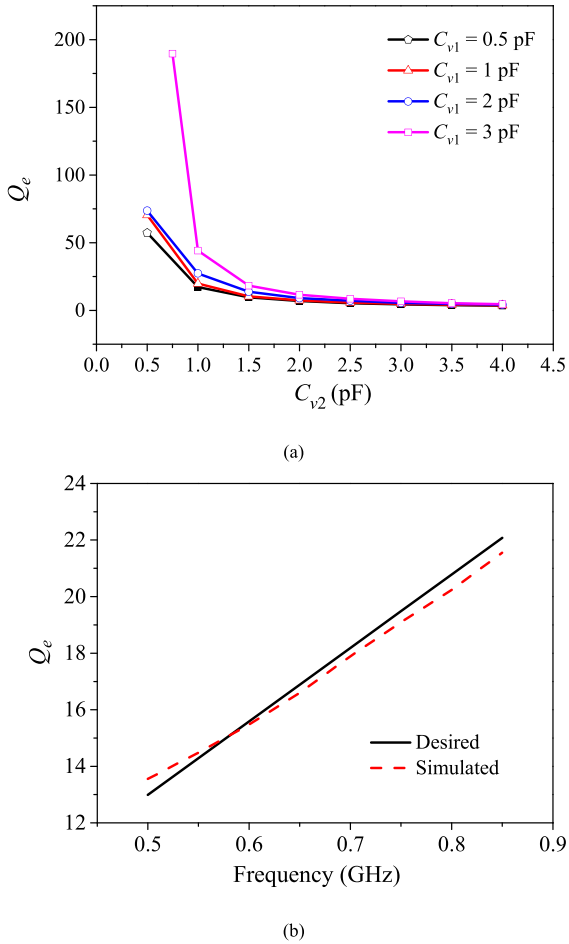

FIGURE 5. The extracted and desired Q_e.(a) extracted Q_e under different C_{v1} and C_{v2}, (b) desired and simulated Q_e under different frequency.

where f_{p2} and f_{p1} represent the lower and higher split resonant frequencies, respectively. By parameters' study, the extracted K_{12} under different coupling regions is plotted in Fig. 4. As expected, K_{12} is mainly affected by the coupling region between the two coupled UIRs. It is obvious that$g$ mainly affects the value of K_{12} while L_1, L_2 and L_3 can effectively change the value and variation trade of K_{12} against the passband frequency. After optimization, $L_1 = 10.8$ mm, $L_2 = 13$ mm, $L_3 = 15$ mm and $g = 0.7$ mm are chosen to construct the coupling region which can make K_{12} close to the desired one in the whole frequency-tuning range.

To achieve the desired Q_e, C_{v2} is added between the feedline and the UIR to tune the Q_e when C_{v1} changes. In order to clearly show the relationship between Q_e and C_{v2}, the Q_e versus different C_{v2} and C_{v1} are extracted by Equation 6, as shown in Fig. 5 (a).

$$Q_e = \frac{f_0}{f_{0\pm 90^\circ}} \tag{6}$$

where f_0 and $f_{0\pm 90^\circ}$ represent the center frequency and the $\pm 90^\circ$ bandwidth with respect to the absolute phase at f_0, respectively.

As can be seen, Q_e can be fully controlled by tuning C_{v2} when C_{v1} changes. By adjusting C_{v2}, the extracted Q_e can be close to the desired one in the whole frequency-tuning range, as shown in Fig. 5(b).

As a result, when the values of K_{12} and Q_e are both close to the desired ones, the proposed filter can realize constant ABW during the whole frequency-tuning process.

B. TWO TRANSMISSION ZEROES OF THE FILTER

As is well known that introducing the S-L coupling between the feeding line is an effective way to realize two TZs for improving the selectivity. In this design, two coupled shunt stubs are employed to realize the S-L coupling (M_{SL}), as shown in Fig. 3. The two TZs can be synthesized by the coupling matrix [39].

By substituting the desired Q_e and K_{12} under different passband frequency into coupling matrix, the desired elements (M_{S1}, M_{12}, and M_{2L}) can be obtained. Subsequently, the desired S-L coupling M_{SL} under different frequency can be calculated, as in Fig. 6. Similarly, when the extracted M_{SL} is close to the desired one, the desired two TZs can be obtained. The coupling level of S-L coupling is mainly

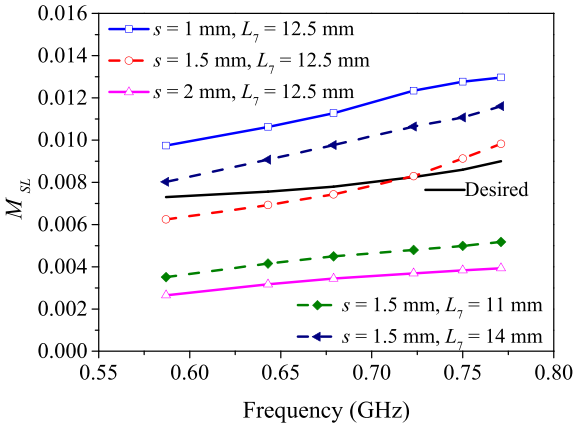

FIGURE 6. Desired and extracted M_{SL} under different s and L_7.

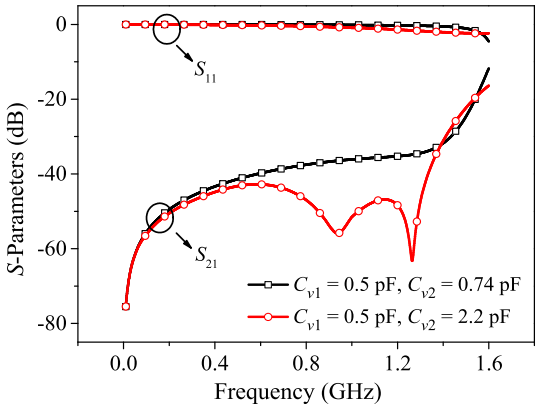

FIGURE 8. The simulated S-parameters under different C_{v2} while $C_{v1} = 0.5$ pF is fixed in the OFF-state.

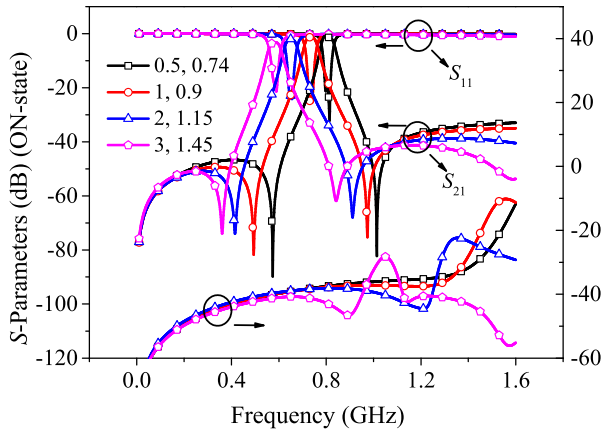

FIGURE 7. The simulated results of reconfigurable filter in ON- and OFF-state. (The inserted numbers represent the capcitance 'C_{v1} (pF), C_{v2} (pF)'.)

determined by its coupling region (i.e., L_7 and s in Fig. 3). By studying these two parameters, the variation of M_{SL} can be extracted, as shown in Fig. 6. As can be seen, M_{SL} can be tuned by adjusting L_7 and s to approach the desired one across the frequency-tuning range. As a result, two desired TZs will be generated and move along the tunable passband.

According to the above discussion, the tunable passband with constant ABW and two TZs can be obtained as shown in Fig. 7.

IV. DESIGN OF THE SWITCHABLITY

When the bias voltage V_p of the PIN is set as 0.8V, the PIN is turned on and the end of UIR is shorted to ground. Hence, in the frequency tuning process of the ON-state passband, once the PIN is turned on, the passband will be switch off (OFF-state). Fig. 7 shows the two-state S-parameters during the frequency tuning process. As can be seen, the tunable passband at any frequency controlled by C_{v1} and C_{v2} can be well turned off. The simulated in-band isolation in the frequency range of interest is better than 37dB.

It is clear that there are two transmission paths for the RF signals in the OFF-state of the passband. The first is the S-L coupling and the second is resonator coupling between the UIRs with two short ends. Thus, the C_{v2} in the second path, which is used to tune the Q_e of the ON-state passband as in Section III, is also useful to improve the isolation. To clearly show the improvement, the OFF-state passband operating at highest frequency (0.8GHz) in Fig. 7 (the black solid line with square symbol) is chosen to be optimized by C_{v2} as shown in Fig. 8. As can be seen, the in-band isolation is improved about 10 dB at 0.8GHz (from 37.4dB to 47.3dB) when C_{v2} is tuned from 0.74 pF to 2.2 pF. Thus, good in-band isolation can be obtained in frequency range of interest by tuning C_{v2}. Therefore, the tunable C_{v2} plays a dual-function role in the two states, i.e. Q_e controlling for the ON-state tunable passband, and isolation improvement for the OFF-state of the passband.

V. RESUITS AND DISCUSSION

According to the discussion above, the dimensions of the demonstrated reconfigurable filter can be optimized as: $W_1 = 1.2$ mm, $W_2 = 0.4$ mm, $W_3 = 1$mm, $W_4 = 1.8$mm, $L_1 = 10.8$ mm, $L_2 = 13$ mm, $L_3 = 15$ mm, $L_4 = 7.4$ mm, $L_5 = 7.7$ mm, $L_6 = 3.6$ mm, $L_7 = 12.5$ mm, $s = 1.5$ mm, $C_p = 33$ pF. The varactor JDV2S71E from Toshiba, which possesses the capacitance range of 0.6-7pF, is employed to realized C_{ai}. The lumped capacitors are chosen as $C_{b1} = 5$ pF and $C_{b2} = 10$ pF. The PIN diodes used in this design are implemented with Skyworks SMP 1345-079LF. The simulation is conducted by using the full-wave simulator HFSS. The measurement is carried out by the Agilent N5230A network analyzer.

Fig. 9 shows the photograph of the fabricated reconfigurable filter. Fig. 10 indicates the simulated and measured results when $V_p = 0$ V (ON-State of the passband), showing good agreement. The used DC bias voltage V_{ci} in the measurement are $V_{c1} = 30$-0 V and $V_{c2} = 11.1$-5.5 V. As a result, the measured passband frequency can be tuned from 0.785 to 0.566 GHz, i.e. frequency-tuning range = 32.4%. Since the specific position of C_{v1} is carefully chosen, as discussed in Section II, the upper stopband is always wide and no spurious

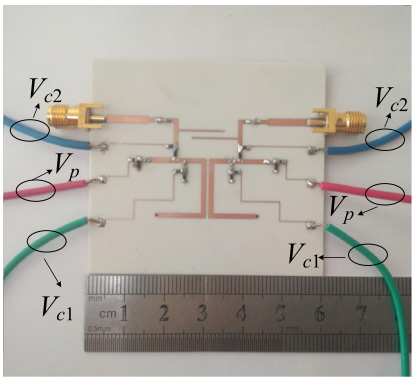

FIGURE 9. Photograph of the fabricated reconfigurable filter.

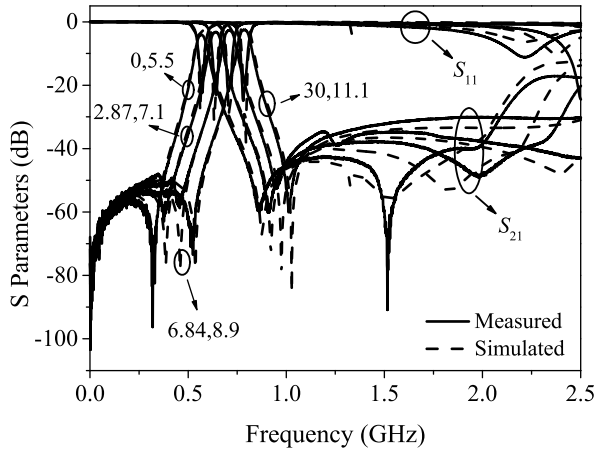

FIGURE 10. Simulated and measured results of the proposed reconfigurable filter when PIN is turned off (V_p = 0 V). (The inserted numbers represent the bias voltage 'V_{c1} (V), V_{c2} (V)'.)

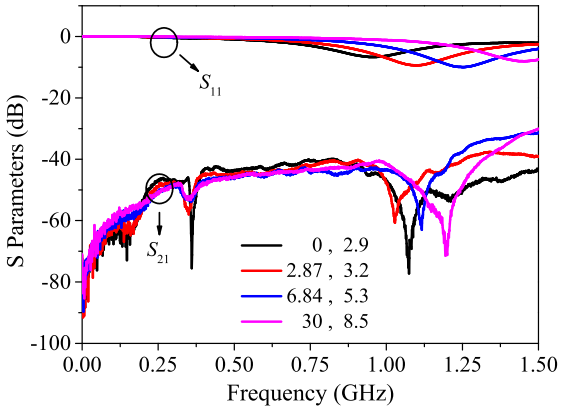

FIGURE 11. The optimized measurement results when the filter works in the OFF-state (V_p = 0.8 V) (The inserted numbers represent the DC bias voltage 'V_{c1} (V), V_{c2} (V)').

TABLE 2. The measured results of the proposed filter.

Bias voltage (ON-state)	V_{c1}=0V, V_{c2}=5.5V	V_{c1}=2.87V, V_{c2}=7.1V	V_{c1}=6.84 V, V_{c2}=8.9V	V_{c1}=30V, V_{c2}=11.1V
f_1 (GHz)	0.566	0.639	0.71	0.785
3-dB ABW (MHz)	49	51.5	52	53
IL (dB)	4.08	3.2	2.7	2.52
Two TZs (GHz)	0.322/0.864	0.531/0.911	0.455/0.951	0.538/1.011
Bias voltage (OFF-state)	V_{c1}=0V, V_{c2}=2.9V	V_{c1}=2.87V, V_{c2}=3.2V	V_{c1}=6.84 V, V_{c2}=5.3V	V_{c1}=30V, V_{c2}=8.5V
Isolation (in-band)	43dB	43.5dB	43.8dB	43.3dB

TABLE 3. Comparison with previous microstrip reconfigurable filters.

	Passband state	IL (dB)	Passband Isolation in OFF-state	Self-adaptive TZs
[30]	Tunable	1.6-4.1	-	Yes
		1.6-3.9	-	Yes
[31]	Switchable	3.05/3.1	55.2dB/ 37.5dB	No
[32]	Switchable	3.4	47dB	No
		3.9	65 dB	No
		3.6	47 dB	No
[35]	Tunable	3.02-4.8/ 2.78-4.6	-	No
[36]	Tunable	1.8-4.6	-	No
This work	Tunable + switchable	2.52-4.08	>43 dB	Yes

appears below 2GHz because the tuning range of f_3 is small as in Fig. 2 and Table 1. The slight difference between the calculated and measured tuning range mainly comes from the model inaccuracy and parasitic elements of the varactor and PIN. In the entire frequency-tuning range, the 3-dB ABW of the tunable passband is within 51 $\pm$ 2 MHz. The fluctuation of 3-dB ABW results from the slight difference between the desired and actual values of K_{12} and Q_e, as shown in Figs. 4 and 5. The passband insertion loss (IL) is within 2.52 - 4.08dB. Meanwhile, two TZs in the lower and higher stopbands are accomplished and move along the tunable passband.

Fig. 11 indicates the measured results when V_p = 0.8 V (the passband is in the OFF-state). As can be seen, when the used DC bias voltage V_{ci} are V_{c1} = 30-0 V and V_{c2} = 8.5-2.9 V, the measured isolation in the whole frequency-tuning range is better than 40dB. Table 2 summarizes the detailed performance of the proposed reconfigurable BPF, which shows stable and high selectivity in the ON-State and high isolation in the OFF-State.

Table 3 summarizes the comparison of the proposed design with the previous reconfigurable filters. As can be seen, the proposed reconfigurable filter has more functions and good performance, such as simultaneously tunable and switchable passband and high selectivity resulting from two self-adaptive TZs. It is well known that the passband IL of the reconfigurable filter mainly is dependent on the parasitic resistance of the diode. Though the proposed design employs four varactors and two PIN diodes, the IL of the proposed design in the range of 2.52-4.08dB is comparable to the previous reconfigurable designs.

VI. CONCLUSION

In this paper, a novel reconfigurable filter with simultaneously tunable and switchable passband has been presented. The tunability and switchability can be both realized in one resonator by using the new loading scheme. The design procedures of the reconfigurable filter in the ON- and OFF-states are given in detailed. In the ON-state, frequency-tunable passband with constant ABW and two accompanying TZs are realized. The varactor in the feeding network, which is employed to control Q_e can also be used to optimize the isolation in the OFF-state. The filter has been fabricated and measured. Good agreement of simulated and measured results show that the proposed reconfigurable filter features multifunctional reconfigurability, constant ABW, high selectivity and high isolation, which would make the proposed reconfigurable solution attractive in the application of modern and future communication systems.

REFERENCES

[1] C. Zhu, J. Xu, W. Kang, and W. Wu, "Microstrip multifunctional reconfigurable wideband filtering power divider with tunable center frequency, bandwidth, and power division," *IEEE Trans. Microw. Theory Techn.*, vol. 66, no. 6, pp. 2800–2813, Jun. 2018.

[2] B. Lee, B. Koh, S. Nam, T.-H. Lee, and J. Lee, "Frequency-tunable filtering power divider with new topology," *IEEE Trans. Compon., Packag., Manuf. Technol.*, vol. 7, no. 7, pp. 1151–1162, Jul. 2017.

[3] L. Yao, Y. Wu, M. Li, W. Wang, and Y. Liu, "Bandwidth-tunable filtering balun based on compact 3D configuration," *Electron. Lett.*, vol. 55, no. 1, pp. 32–34, Jan. 2019.

[4] Z. Zhuang, Y. Wu, Y. Liu, and Z. Ghassemlooy, "Wideband bandpass-to-all-stop reconfigurable filtering power divider with bandwidth control and all-passband isolation," *IET Microw. Antennas Propag.*, vol. 12, no. 11, pp. 1852–1858, Sep. 2018.

[5] H. Liu, S. Fang, and Z. Wang, "A compact trans-directional coupler with wide frequency tuning range and superior performance," *IEEE Trans. Compon., Packag., Manuf. Technol.*, vol. 7, no. 10, pp. 1670–1677, Oct. 2017.

[6] Y. F. Pan, S. Y. Zheng, Y. M. Pan, Y. X. Li, and Y. L. Long, "Highly reconfigurable dual-band coupler with independently tunable operating frequencies," *IEEE Trans. Ind. Electron.*, vol. 66, no. 5, pp. 3615–3626, May 2019.

[7] T. Yang and G. M. Rebeiz, "A simple and effective method for 1.9–3.4-GHz tunable diplexer with compact size and constant fractional bandwidth," *IEEE Trans. Microw. Theory Techn.*, vol. 62, no. 2, pp. 436–449, Feb. 2016.

[8] L. Ge and K. M. Luk, "Band-reconfigurable unidirectional antenna: A simple, efficient magneto-electric antenna for cognitive radio applications," *IEEE Antennas Propag. Mag.*, vol. 58, no. 2, pp. 18–27, Apr. 2016.

[9] R. L. Haupt and M. Lanagan, "Reconfigurable antennas," *IEEE Antennas Propag. Mag.*, vol. 55, no. 1, pp. 49–61, Feb. 2013.

[10] M. Rais-Zadeh, J. T. Fox, D. D. Wentzloff, and Y. B. Gianchandani, "Reconfigurable radios: A possible solution to reduce entry costs in wireless phones," *Proc. IEEE*, vol. 103, no. 3, pp. 438–451, Mar. 2015.

[11] P. Wong and I. C. Hunter, "Electronically reconfigurable microwave bandpass filter," *IEEE Trans. Microw. Theory Techn.*, vol. 57, no. 12, pp. 3070–3079, Dec. 2009.

[12] N. Kumar and Y. K. Singh, "Compact tunable low-pass to CFBW bandpass switchable filter using concentric resonators," *IET Microw., Antennas Propag.*, vol. 12, no. 14, pp. 2225–2233, Nov. 2018.

[13] N. Kumar and Y. K. Singh, "RF-MEMS-based bandpass-to-bandstop switchable single- and dual-band filters with variable FBW and reconfigurable selectivity," *IEEE Trans. Microw. Theory Techn.*, vol. 65, no. 10, pp. 3824–3837, Oct. 2017.

[14] T. Yang and G. M. Rebeiz, "Bandpass-to-bandstop reconfigurable tunable filters with frequency and bandwidth controls," *IEEE Trans. Microw. Theory Techn.*, vol. 65, no. 7, pp. 2288–2297, Jul. 2017.

[15] H. Jiang, B. Lacroix, K. Choi, Y. Wang, A. T. Hunt, and J. Papapolymerou, "*Ka*-and *U*-band tunable bandpass filters using ferroelectric capacitors," *IEEE Trans. Microw. Theory Techn.*, vol. 59, no. 12, pp. 3068–3074, Dec. 2011.

[16] S. Courreges, Y. Li, Z. Zhao, K. Choi, A. Hunt, and J. Papapolymerou, "Two-pole *X* -band-tunable ferroelectric filters with tunable center frequency, fractional bandwidth, and return loss," *IEEE Trans. Microw. Theory Techn.*, vol. 57, no. 12, pp. 2872–2881, Dec. 2009.

[17] N. Vahabisani, S. Khan, and M. Daneshmand, "Microfluidically reconfigurable rectangular waveguide filter using liquid metal posts," *IEEE Microw. Wireless Compon. Lett.*, vol. 26, no. 10, pp. 801–803, Oct. 2016.

[18] P. Wong and I. Hunter, "Electronically tunable filters," *IEEE Microw. Mag.*, vol. 10, no. 1, pp. 46–54, Jan. 2009.

[19] X. Y. Zhang, C. H. Chan, Q. Xue, and B. J. Hu, "RF tunable bandstop filters with constant bandwidth based on a doublet configuration," *IEEE Trans. Ind. Electron.*, vol. 59, no. 2, pp. 1257–1265, Feb. 2012.

[20] J.-X. Chen, Y. L. Ma, J. Cai, L.-H. Zhou, Z.-H. Bao, and W. Q. Che, "Novel frequency-agile bandpass filter with wide tuning range and spurious suppression," *IEEE Trans. Ind. Electron.*, vol. 62, no. 10, pp. 6428–6435, Oct. 2015.

[21] H.-Y. Tsai, T.-Y. Huang, and R.-B. Wu, "Varactor-tuned compact dual-mode tunable filter with constant passband characteristics," *IEEE Trans. Compon., Packag., Manuf. Technol.*, vol. 6, no. 9, pp. 1399–1407, Sep. 2016.

[22] C.-X. Zhou, C.-M. Zhu, and W. Wu, "Tunable dual-band filter based on stub-capacitor-loaded half-mode substrate integrated waveguide," *IEEE Trans. Microw. Theory Techn.*, vol. 65, no. 1, pp. 147–155, Jan. 2017.

[23] D. Psychogiou and R. Gómez-García, "Multi-mode-cavity-resonator-based bandpass filters with multiple levels of transfer-function adaptivity," *IEEE Access*, vol. 7, pp. 24759–24765, 2019.

[24] X. Y. Zhang, J.-X. Xu, and J.-X. Chen, "High-power filtering switch with low loss and high isolation based on dielectric resonator," *IEEE Trans. Microw. Theory Techn.*, vol. 65, no. 6, pp. 2101–2110, Jun. 2017.

[25] D. Psychogiou, R. Gómez-García, and D. Peroulis, "Single and multiband acoustic-wave-lumped- element-resonator (AWLR) bandpass filters with reconfigurable transfer function," *IEEE Trans. Microw. Theory Techn.*, vol. 64, no. 12, pp. 4394–4404, Dec. 2016.

[26] R. Gómez-García, J. Muñoz-Ferreras, J. Jimenéz-Campillo, F. Branca-Roncati, and P. Martín-Iglesias, "High-order planar bandpass filters with electronically-reconfigurable passband width and flatness based on adaptive multi-resonator cascades," *IEEE Access*, vol. 7, pp. 11010–11019, 2019.

[27] B. Li, Y. Wu, C. Yu, and Y. Liu, "Independently tunable concurrent dual-band VCO using square open-loop resonator," *IEEE Access*, vol. 6, pp. 12634–12641, 2018.

[28] C.-W. Tang, C.-T. Tseng, and S.-C. Chang, "Design of the compact tunable filter with modified coupled lines," *IEEE Trans. Compon., Packag., Manuf. Technol.*, vol. 4, no. 11, pp. 1815–1821, Nov. 2014.

[29] J.-X. Chen, M.-Z. Du, Y.-L. Li, Y.-J. Yang, and J. Shi, "Independently tunable/controllable differential dual-band bandpass filters using element-loaded stepped-impedance resonators," *IEEE Trans. Compon., Packag., Manuf. Technol.*, vol. 8, no. 1, pp. 113–120, Jan. 2018.

[30] X. Y. Zhang and Q. Xue, "High-selectivity tunable bandpass filters with harmonic suppression," *IEEE Trans. Microw. Theory Techn.*, vol. 58, no. 4, pp. 964–969, Apr. 2010.

[31] P.-H. Deng and J.-H. Jeng, "A switched reconfigurable high-isolation dual-band bandpass filter," *IEEE Microw. Wireless Compon. Lett.*, vol. 21, no. 2, pp. 71–73, Feb. 2011.

[32] S.-F. Chao, C.-H. Wu, Z.-M. Tsai, H. Wang, and C. H. Chen, "Electronically switchable bandpass filters using loaded stepped-impedance resonators," *IEEE Trans. Microw. Theory Techn.*, vol. 54, no. 12, pp. 4193–4201, Dec. 2006.

[33] C.-F. Chen, G.-Y. Wang, and J.-J. Li, "Microstrip switchable and fully tunable bandpass filter with continuous frequency tuning range," *IEEE Microw. Wireless Compon. Lett.*, vol. 28, no. 6, pp. 500–502, Jun. 2018.

[34] F.-C. Chen, R.-S. Li, and J.-P. Chen, "A tunable dual-band bandpass-to-bandstop filter using p-i-n diodes and varactors," *IEEE Access*, vol. 6, pp. 46058–46065, 2018.

[35] G. Chaudhary, Y. Jeong, and J. Lim, "Dual-band bandpass filter with independently tunable center frequencies and bandwidths," *IEEE Trans. Microw. Theory Techn.*, vol. 61, no. 1, pp. 107–116, Jan. 2013.

[36] H. Zhu and A. M. Abbosh, "Tunable balanced bandpass filter with wide tuning range of center frequency and bandwidth using compact coupled-line resonator," *IEEE Microw. Wireless Compon. Lett.*, vol. 26, no. 1, pp. 7–9, Jan. 2016.
[37] J.-X. Chen, Y.-J. Zhang, J. Cai, Y.-L. Li, and Y.-J. Yang, "Overall study of frequency-agile mechanism of varactor-loaded λ/4 resonator for designing tunable filter with stable wide stopband," *IEEE Trans. Ind. Electron.*, vol. 66, no. 8, pp. 6302–6310, Aug. 2019.
[38] X. Y. Zhang, Q. Xue, C. H. Chan, and B. J. Hu, "Low-loss frequency-agile bandpass filters with controllable bandwidth and suppressed second harmonic," *IEEE Trans. Microw. Theory Techn.*, vol. 58, no. 6, pp. 1557–1564, Jun. 2010.
[39] J. Cai, J.-X. Chen, X.-F. Zhang, Y.-J. Yang, and Z.-H. Bao, "Electrically varactor-tuned bandpass filter with constant bandwidth and self-adaptive transmission zeros," *IET Microw. Antenna Propag.*, vol. 11, no. 11, pp. 1542–1548, Sep. 2017.

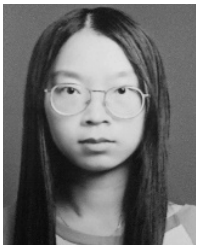

YU-JING ZHANG was born in Nantong, Jiangsu, China, in 1995. She received the B.Sc. degree in electronic science and technology from Nantong University, Nantong, China, in 2017, where she is currently pursuing the M.Sc. degree in electromagnetic field and microwave technology. Her current research interests include microwave passive and reconfigurable filters.

JING CAI was born in Nantong, Jiangsu, China, in 1992. He received the B.Sc. degree in biomedical engineering and the M.Sc. degree in information and communication engineering from Nantong University, Nantong, China, in 2015 and 2018, respectively. His current research interests include microwave passive and reconfigurable filters.

JIAN-XIN CHEN (M'08–SM'17) was born in Nantong, Jiangsu, China, in 1979. He received the B.S. degree from the Huai Yin Teachers College, Jiangsu, in 2001, the M.S. degree from the University of Electronic Science and Technology of China (UESTC), Chengdu, China, in 2004, and the Ph.D. degree from the City University of Hong Kong, Hong Kong, in 2008. Since 2009, he has been with Nantong University, where he is currently a Professor. He has authored or coauthored more than 80 internationally refereed journal and conference papers. He holds three Chinese patents and two U.S. patents. His research interests include microwave active/passive circuits and antennas, and LTCC-based millimeter-wave circuits and antennas.

Dr. Chen was a recipient of the Best Paper Award presented at the Chinese National Microwave and Millimeter-Wave Symposium, Ningbo, China, in 2007. He was a Supervisor of 2014 iWEM Student Innovation Competition Winner in Sapporo, Japan.